JOURNAL OF MATERIALS SCIENCE **34** (1999) 599–606

Ausforming of NiTi

E. HORNBOGEN
Ruhr-Universität, D-44801 Bochum, Germany
E-mail: erhard.hornbogen@rz.ruhr-uni-bochum.de

Lattice defects are introduced into stable austenite (β) by hot rolling up to 70% (in one pass) in a temperature range between $900 > T_{AF} > 340\,^{\circ}$C (ausforming (AF)). The changes in microstructure, thermal transformation behavior, as well as normal and anomalous properties in stress-, strain-, and temperature-space were studied. Martensitic transformation temperatures are lowered with decreasing deformation temperature and increasing amount of deformation. A two-stage reaction is induced at $T_{AF} \leq 400\,^{\circ}$C. Deformation twins are the predominant microstructural feature, in addition to dislocations at $T_{AF} \leq 700\,^{\circ}$C. Highly elongated grains indicate that long-range recrystallization is absent at all ausforming temperatures. Semicoherent pecipitation in addition to high dislocation densities are likely to be responsible for the premartensitic anomalies of thermal transformation for $T_{AF} \leq 400\,^{\circ}$C. Ausforming leads to a considerable increase in conventional strength properties (yield stress, tensile strength, elongation) without loss of transformability and, consequently, shape memory or pseudo-elasticity.

List of Symbols and Units

Symbol	Unit	Meaning
$A \equiv \beta$	–	Austenite
AF	–	Ausforming
b, b_α, b_β	m	Burger's vector
C_α, C_β	l	Relating defect distribution to $\Delta\sigma$
ε	l	Any strain
ε_{AF}	l	Amount of ausforming
$\varepsilon_{e\alpha}$, $\varepsilon_{e\beta}$	l	Elastic deformation in α, β
$\varepsilon_{p\alpha}$, $\varepsilon_{p\beta}$	l	Plastic deformation in α, β
$\varepsilon_{\beta\alpha}$	l	Strain due to $\beta \rightarrow \alpha$ transformation
$\varepsilon_{f\alpha}$	l	Fracture strain in martensite α
G_α, G_β	Pa	Shear modulus of α, β
$\gamma_{\beta\alpha}$	l	$\beta\alpha$ transformation shear
$M \equiv \alpha$	–	Martensite
M_s	K	Martensite start
ΔM_s (AF)	K	Change of M_s due to AF
M_d	K	Limit of strain-induced M-formation
$R_{p\alpha}$	Pa	Yield stress
$R_{m\alpha}$	Pa	Tensile strength
ϱ_α, ϱ_β	m^{-2}	Defect density in α, β (dislocations)
$S_{\beta\alpha}$	$J\,K^{-1}\,m^{-3}$	Entropy of $\beta \rightarrow \alpha$ transformation
σ	Pa	Any stress
$\sigma_{\beta\alpha}$	Pa	Stress for $\beta \rightarrow \alpha$ transformation
$\sigma_{\beta\alpha S}$, $\sigma_{\beta\alpha f}$	Pa	Start, finish of transformation
$\Delta\sigma_{\beta\alpha}$ (AF)	Pa	Raise of $\sigma_{\beta\alpha}$ due to AF
T	K	Any temperature
T_{AF}	K	Ausforming temperature: $T > M_d$

1. Introduction

The term "ausforming" was first used for a thermomechanical treatment (TMT) by which defects were introduced into the austenitic structure of certain steels [1]. Subsequent martensitic transformation of defect austenite in maraging steels may lead to ultra high yield strengths of >3 GPa [2]. In this case, the austenite is deformed in a temperature range of metastability between pearlite and bainite, above the temperature (M_d) below which strain- or stress-induced transformation takes place. Strengthening is due to the fact that additional lattice defects, especially dislocations, are sheared into the martensite during cooling from the deformation temperature.

More recently, this method was applied to brass-type shape memory alloys (SMA) [3]. The purpose is again an improvement of strength, while shape memory is expected to be preserved or improved [4]. In addition to better load carrying ability, an enhanced resistance to thermomechanical fatigue is often required for shape memory applications [5].

Six temperature ranges can be defined for which shape memory alloys show different deformation behavior under mechanical stress (Fig. 1). Ausforming has to take place in untransforming homogeneous austenite, range I, in which small amounts of a second phase may form (range 1C), for example

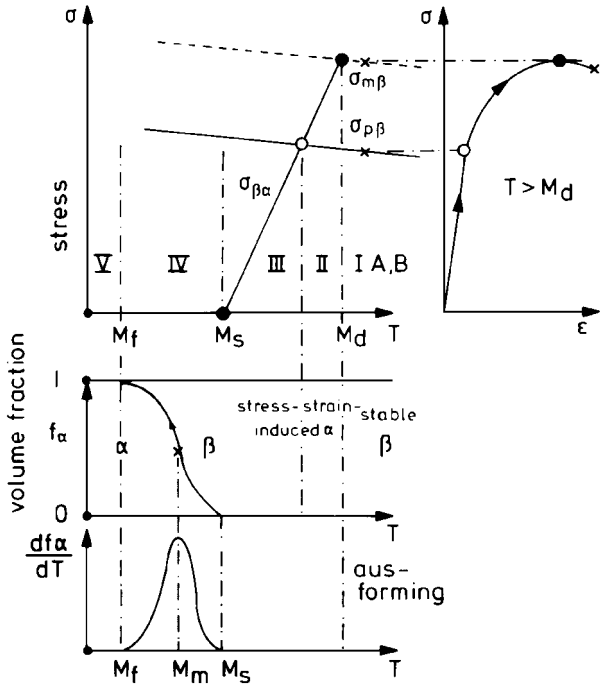

Figure 1 Definition of temperature ranges for deformation of alloys which undergo martensitic transformation below M_s: $T_I < M_d$ plastic deformation of stable austenite β; (a) disordered solid solution; (b) ordered intermetallic compound and (c) heterogeneous structure. $T_{III} < T_{II} < M_d$ plastic strain (in β) induced $\beta \rightarrow \alpha$ transformation; $M_\varrho < T_{III} < T_{II}$ stress-induced $\beta \rightarrow \alpha$ transformation; $M_f < T_{IV} < M_s$ continued stress-induced $\beta \rightarrow \alpha$ plus reorientation $\alpha^{+-} \rightarrow \alpha^{+}$ of $(\beta + \alpha)$ phase mixture; $T_V < M_f$ reorientation of completely transformed domain structure $\alpha^{+-} \rightarrow \alpha^{+}$, disordering by high amounts of deformation; M_m temperature of maximum rate of martensitic formation during cooling corresponds to the maxima in the DSC-curves (see Figs 3b, 4c, 6c): $df\alpha/dt = \max$.

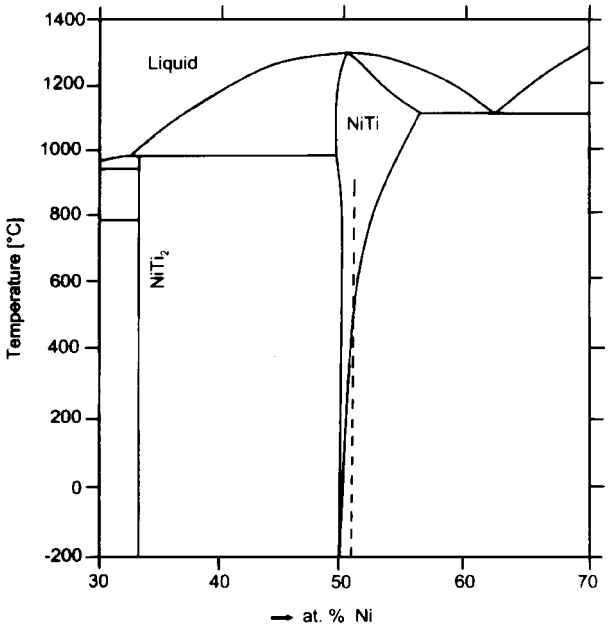

Figure 2 Section of the NiTi-phase-diagram indicating the composition of the alloy (dotted).

by precipitation (ausageing). In Cu-base alloys an order → disorder transformation takes place around 500 °C so that pure ausforming (range I) implies introduction of $^a/_2\ \langle 1\,1\,1\rangle$ dislocations into the b.c.c.-lattice [4]. The present paper is concerned with slightly off-stochiometric NiTi, which provides the prerequisite for precipitation at $T < 500\,^\circ$C, and which—in contrast to the Cu-base alloys—remains ordered up to the melting temperauture (∼1200 °C) (Fig. 2).

The purpose of this investigation is the analysis of the effect of defects introduced into austenite on thermal or mechanical martensitic transformation behavior and on conventional strength.

2. Material and experimental procedure

The chemical composition of the alloy was slightly off-stochiometric, 50.3 at % Ni (Figs 1 and 2), so that precipitation could be expected for $T < 500\,^\circ$C. The course of the transformation cycles, as determined by differential scanning calorinetry (DSC), of the as-received and betatized state agreed rather well. Ausforming (AF) was conducted in a temperature range of $340\,^\circ\text{C} < T_{AF} < 900\,^\circ$C. The deformation could be obtained by rolling and subsequent quenching in one pass (unless otherwise indicated). Amounts of deformation up to about 70% were reached for $T_{AF} \geq 400\,^\circ$C. Plastic deformability decreased considerably at lower temperatures.

DSC was used to analyze thermal transformation cycles of all the TM-treated specimen. Stress-strain curves and mechanical cycles were obtained of selected ausforming treatments. A combination of light microscopy (LM), scanning (SEM) and transmission electron microscopy (TEM) were required for a complete analysis of the microstructure: β-grain structure, martensite morphology and defects introduced into austenite by the AF-treatment.

3. Experimental results

The as-received or the as-betatized conditions of the alloys show the simplest possible (one step) transformation behavior with M_s just below, A_f above ambient temperature (Fig. 3). The grain structure is equi-axed, superimposed is a dispersoid of about 3 vol % of 1 μm diameter particles, possibly TiO_2 introduced during metallurgical processing or TiC, from impurities of carbon of 0.13 wt %. Ambient temperature corresponds to the onset of martensitic transformation. Cooling to $-196\,^\circ$C leads to a fully transformed fine-scale, fractal structure. Ausforming lowers somewhat the temperature range (M_s, M_m, M_f) of martensitic transformation, while retransformation is almost unaffected (Fig. 4). Nevertheless, the LM microstructure is changed considerably into elongated grains, implying no evidence for longrange recrystallization (Fig. 5). In addition, twins appear, increasing in number with amount of deformation and decreasing ausforming temperature, changing orientation from about 45° to parallel to the direction of rolling. These twins can, but must not, be confused with martensitic crystals, because they form far above M_d (Fig. 1). In the total range of $500\,^\circ\text{C} \leq T_{AF} < 900\,^\circ$C, a simple one-step reverse transformation behavior is observed during a colling/heating cycle: A → M → A (Fig. 4).

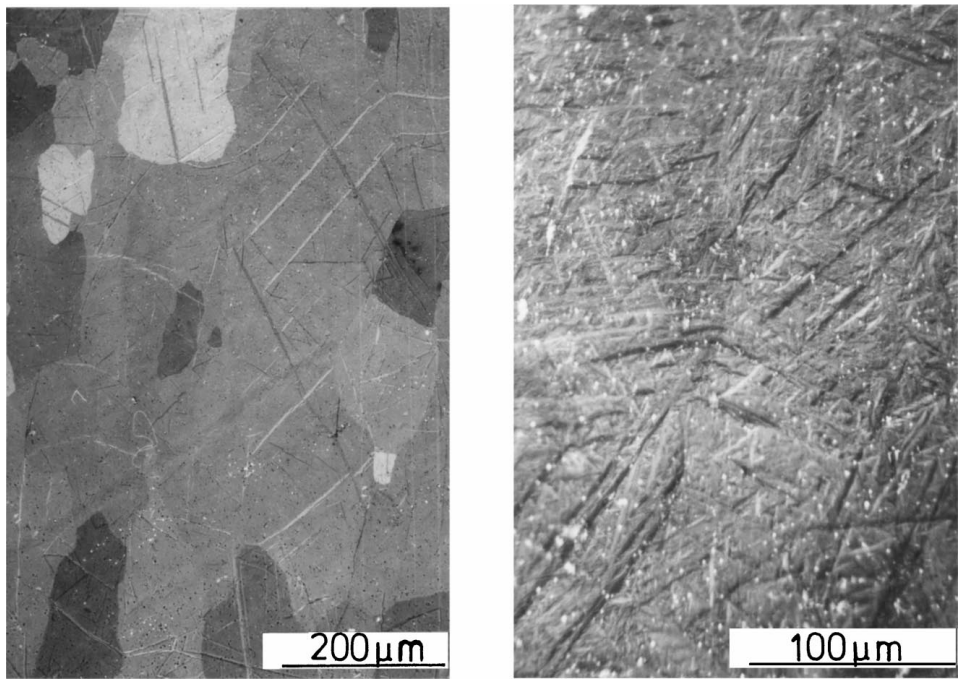

(a)

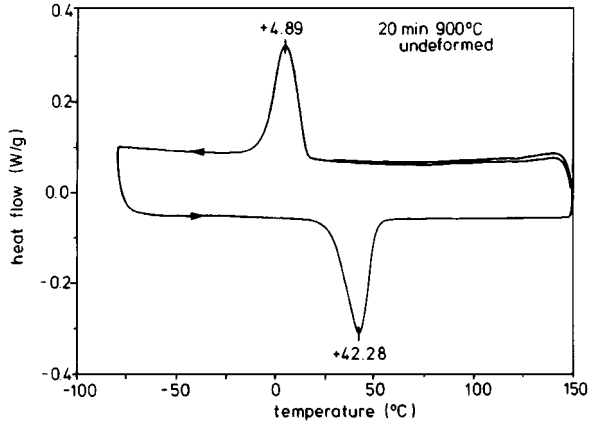

(b)

Figure 3 (a) Microstructure (LM) of undeformed betatized state: 20′ at 900 °C ↓ H_2O (incipient martensite) and after full transformation to −196 °C and reheating to 20 °C (fractal martensite); and (b) DSC reversible single step cycle.

At $T_{AF} = 400\,^{\circ}\mathrm{C}$ only after 70% deformation, and at the lower deformation temperatures a two-stage process is induced. The separation becomes more pronounced with increasing amount of deformation and decreasing temperature (Fig. 6). There are no new features revealed by light microscopy (Fig. 7). Martensitic transformation takes place in the finally twinned microstructure of the ausformed austenite at a fine scale, which can only be resolved by SEM (Fig. 7b and c).

Transmission electron microscopy (TEM) confirms the formation of deformation twins and dislocations in a wide temperature range (Figs 5 and 7), and provides evidence for precipitation at $T_{AF} < 400\,^{\circ}\mathrm{C}$ (Fig. 7).

After microstructural analysis, these structures were studied in σ-, ε-, T-space by tensile and compression tests and heating experiments. All experiments started out in the austenitic condition. The course of a stress-strain curve is composed of five ranges of different types of deformation ε (Fig. 8):

I	$\varepsilon_{e\beta}$	elastic, austenite β;
II	$\varepsilon_{\beta\alpha}$	stress-induced transformation;
III	$\varepsilon_{e\alpha}$	elastic, stress-induced martensite;
IV	$\varepsilon_{p\alpha}$	plastic, martensite;
V	$\varepsilon_{f\alpha}$	fracture of martensite after necking.

Fig. 9 shows the typical course of stress–strain curves and the effects of ausforming. Typical data obtained from tensile tests have been summarized in Table I. Start $\sigma_{\beta\alpha S}$ and finish $\sigma_{\beta\alpha f}$ of stress-induced transformation is shifted to slightly higher stresses. More pronounced is the increase in yield stress $R_{p\alpha}$ and tensile strength R_m. Elongation to fracture is also increased. Fractographic studies by SEM showed ductile simple-fracture in all cases, preceded by uniform elongation which was increased considerably by ausforming. The results obtained by tensile testing were confirmed by a number of compression tests as far as $\sigma_{\beta\alpha}$ and $R_{p\alpha}$ is concerned.

Mechanical cycling experiments showed for comparable conditions, i.e. constant strain of 3%, a higher stability of the ausformed state for mechanical, as well as for mechano-thermal cycles because of the increase in conventional yield stress R_{pa} (Fig. 10).

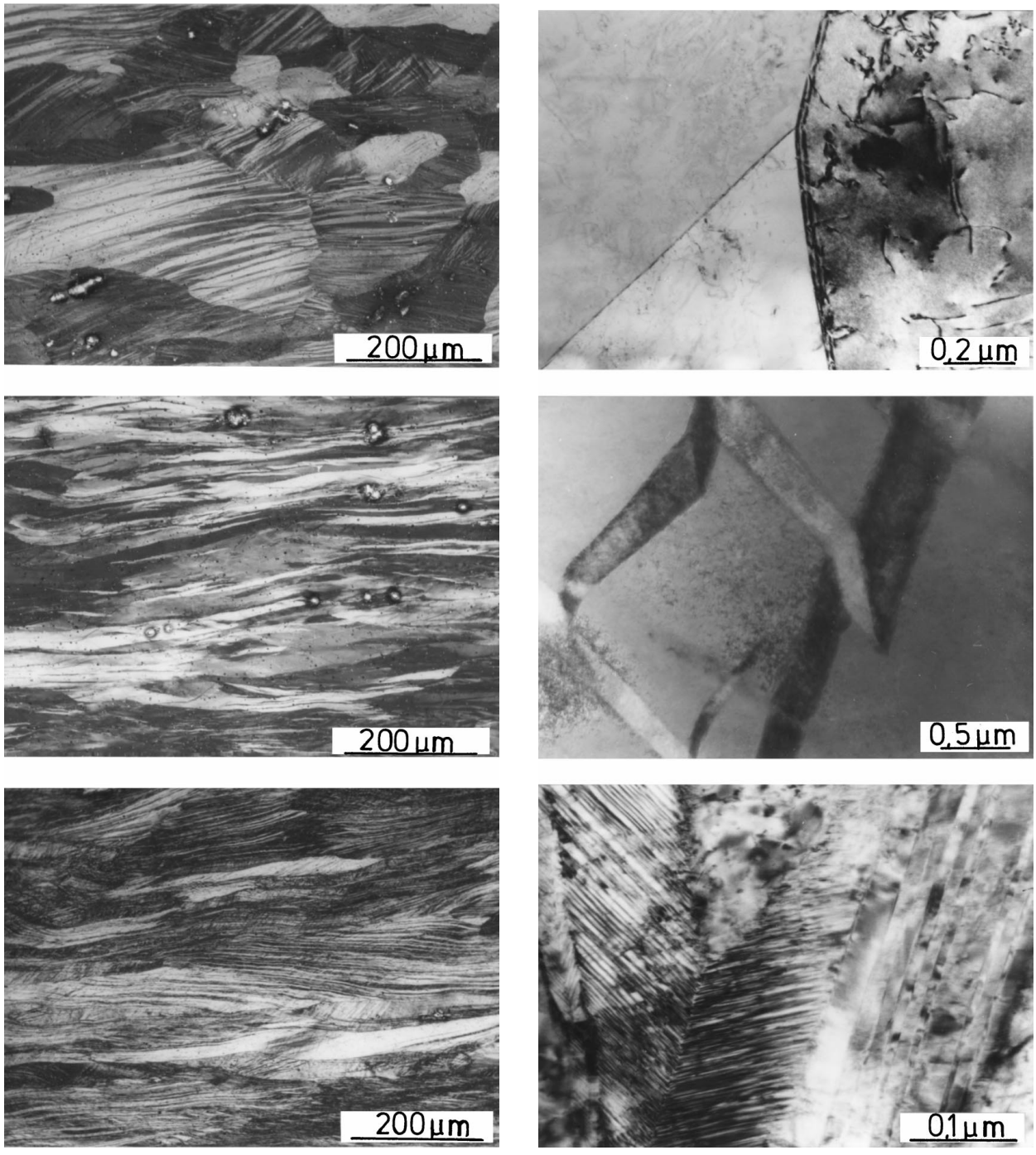

(a) (b)

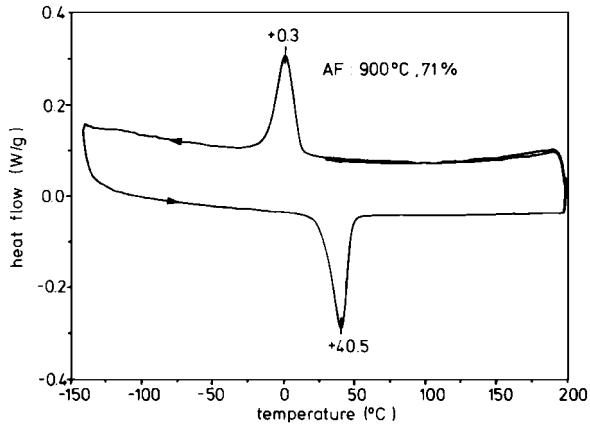

(c)

Figure 4 Ausforming at $T_{AF} \geq 500\,^{\circ}\mathrm{C}$; (a) Light microscopy ($T_{AF}$, ε_{AF}) 1) 500 °C 28% twinned structure 2) 900 °C 71% lamination 3) 500 °C 71% fine lamination; (b) Transmission electron microscopy 1) betatized grain boundaries, dislocation 2) 500 °C 28% deformation interacting with defect structure; and (c) DSC, same type of transformation as Fig. 3b, lowered transformation temperatures.

TABLE I Results of tensile (T) and compression (C) tests

	T/C	$\sigma_{\beta\alpha S}$	$\sigma_{\beta\alpha f}$	ε at $\sigma_{\beta\alpha f}$	$R_{p\alpha}$	ε at $\sigma_{p\alpha}$	R_m	ε_f
Undeformed	T	200	320	5.7	580	+6.8	720	10
400 °C, 30%	T	225	320	6.1	612	+7.8	920	18
400 °C, 65%	T	244	310	5.6	700	+7.5	980	18
400 °C, 75%	T	266	325	5.4	730	+7.5	980	17
Underformed as betatized	C	150	300	−4.4	870	−6.3	–	–
500 °C, 28%	C	160	330	−4.6	1060	−7.2	–	–
500 °C, 71%	C	150	320	−4.8	1080	−7.0	–	–
380 °C, 30%	C	210	390	−4.4	1210	−7.2	–	–

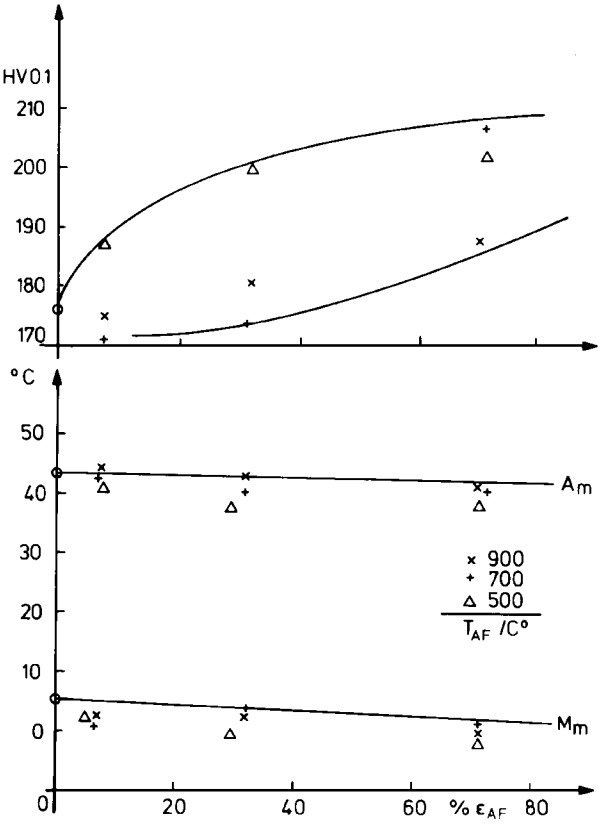

Figure 5 Transformation temperatures (M_m, A_m, see Fig. 1) and hardening as function of amount of ausforming ε_{AF}.

4. Discussion

It is well established that twinning in b.c.c. solid solution is disfavored by order [7], because the nearest neighbor relations must be changed so that twinning in the B2-structure implies formation of a new crystal structure. Slip facilitated by pairs of $a/2\ \langle 1\,1\,1\rangle$ dislocations becomes the easier process [8]. This work has shown that this is not true for elevated temperatures. Evidently a combined "twinning-plus-restoration-of-order" process competes successfully with slip so that the typical twin-lamellated microstructure originates in a wide range of ausforming conditions (Figs 5, 7, 11 and 12).

The major concern of this investigation was how the defect structure of austenite affects thermally and mechanically induced martensitic transformation [9, 10], as well as conventional mechanical properties such as yield stress R_p and tensile strength R_m and true plastic deformability. The twinned microstructure induces a very fine-scale martensite; its amount is hardly reduced. Mainly due to the dislocation forest inside the twins the driving force required for formation of martensite crystals is increased. A consequence is the lowering of the temperature range of martensite formation (M_m maximum rate of formation). The pseudo-yield stress is raised (stress required for the onset of stress-induced $\beta \rightarrow \alpha$ transformation $\sigma_{\beta\alpha S}$). Both effects must be due to the interaction of the partial dislocations in the moving β/α-transformation interface with the defects introduced during ausforming (Fig. 13) [9, 10]:

$$M_S(0) - \Delta M_S(\mathrm{AF}) = M_S$$
$$\Delta M_S(\mathrm{AF}) = \Delta\sigma_{\beta\alpha}\frac{\gamma_{\beta\alpha}}{S_{\beta\alpha}} \tag{1}$$

Conventional strength of austenite would have to be measured above the M_d-temperature (Fig. 1). In this investigation, it was estimated by hardness measurements [6], conducted at somewhat elevated temperature (+100 °C, Figs 4 and 6) to avoid stress induced martensite as well as diffusional relaxation. Strengthening is due to the increased defect density and possibly to a change in texture.

$$\sigma_{\beta\alpha}(0) + \Delta\sigma_{\beta\alpha}(\mathrm{AF}) = \sigma_{\beta\alpha}$$
$$\Delta\sigma_{\beta\alpha}(\mathrm{AF}) = C_\beta G_\beta b_{\beta\alpha}\sqrt{\varrho_\beta} \tag{2}$$

For the analysis of complete stress–strain curves, the five strain ranges are to be distinguished (Figs 8 and 9):

$$\varepsilon = \varepsilon_{e\beta} + \varepsilon_{\beta\alpha} + \varepsilon_{e\alpha} + \varepsilon_{p\alpha} + \varepsilon_{f\alpha} \tag{3}$$

Ausforming considerably affects the stress levels at which the different modes of deformation occur. $\varepsilon_{p\alpha}$ implies (true) plastic deformation of stress-induced martensite which has inherited the ausforming-induced defects. The stress ranges for these different deformations depend differently on temperature (Figs 13 and 14). The plateau stresses $\sigma_{\beta\alpha S}, \sigma_{\beta\alpha f}$ are highly temperature-dependent according to a Clausius–Clapeyron type equation [9]:

$$\frac{d\sigma_{\beta\alpha}}{dT} = \frac{S_{\beta\alpha}}{\gamma_{\beta\alpha}} \tag{4}$$

$\sigma_{\beta\alpha}$ approaches zero at M_s. The yield stress of the stress-induced martensite shows only negligible

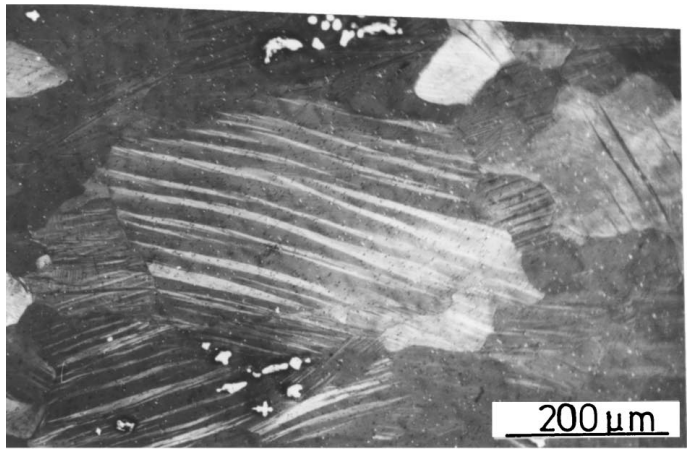

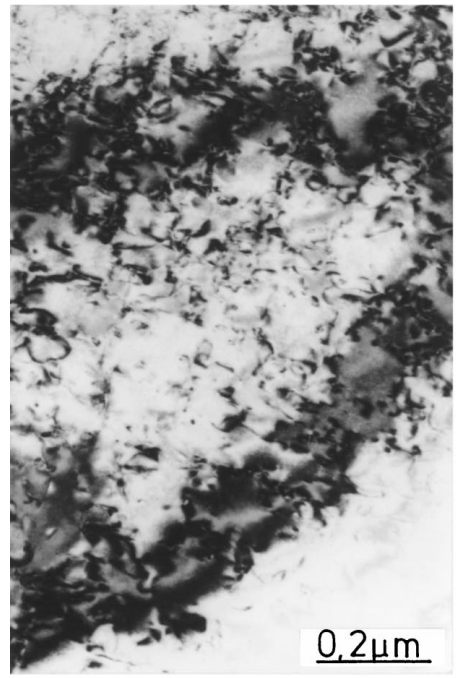

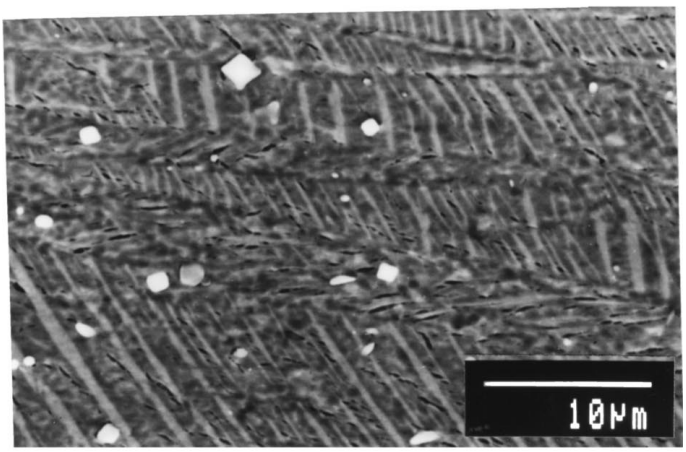

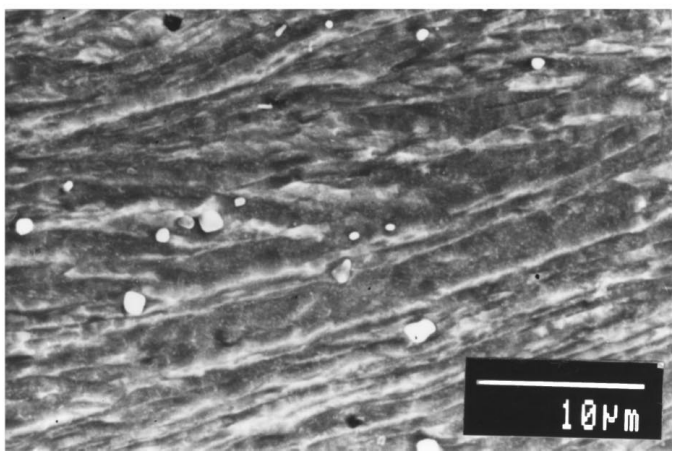

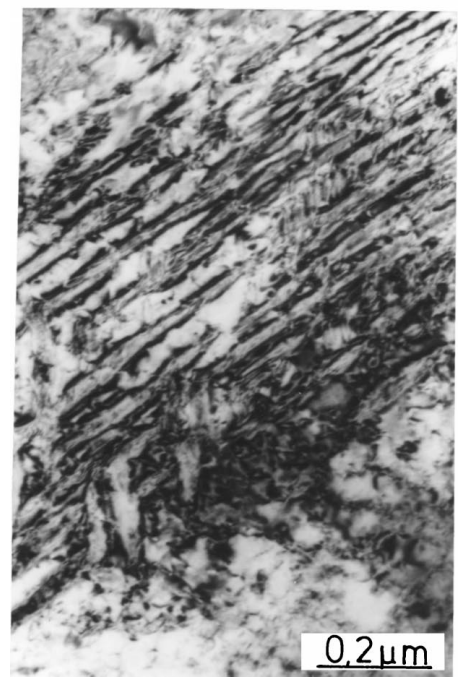

(a) (b)

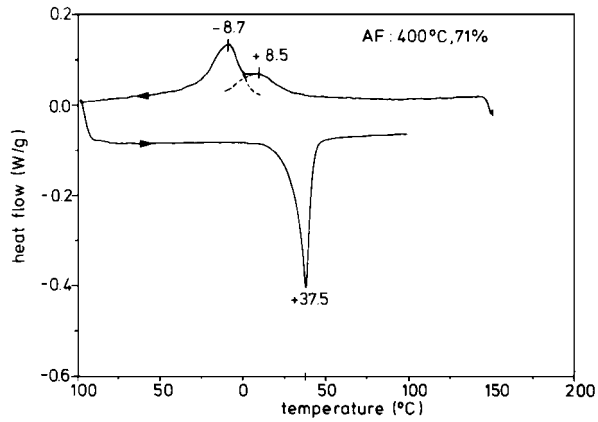

(c)

Figure 6 Ausforming at $T_{AF} < 500\,^{\circ}$C (a) 1) 340 °C 8% twinning in grains (LM) 2) 400 °C 30% cooled to −196 °C, martensite in lamellated structure (SEM) 3) 400 °C 70% cooled to −196 °C, ultra-fine martensite in lamellated structure; (b) 1) 400 °C 30% $\varrho \approx 10^{15}$ m^{-2}, plus particles < 0.1 μm ϕ (TEM-bright field) 2) 400 °C 30% fine scale twinning, dislocations, particles; and (c) DSC two-step reaction during cooling.

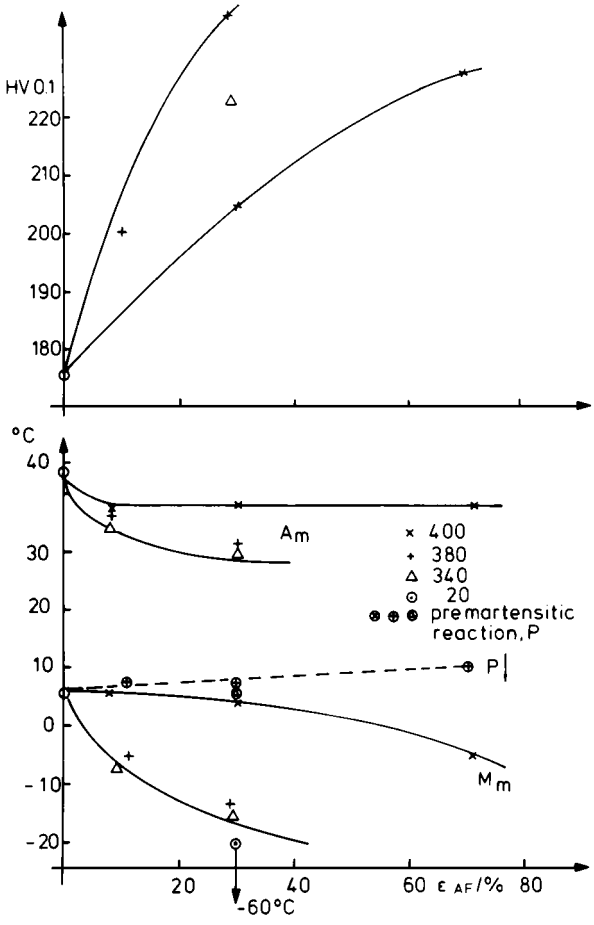

Figure 7 Transformation temperatures (M_m, A_m, premartensitic P) and hardening as functions of amount of ausforming ε_{AF} (⊙ cold worked).

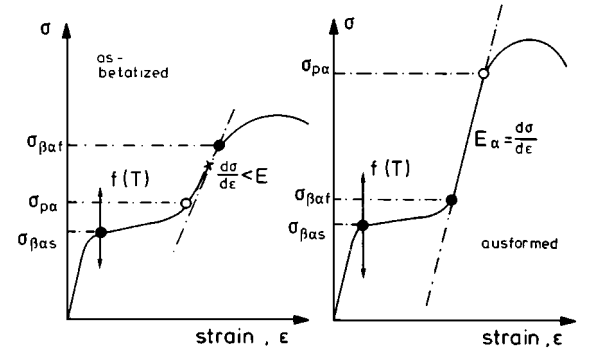

Figure 8 Effects of ausforming on stress-strain curves (test temperature, range T_{III}), schematic: required is finish of transformation $\sigma_{\beta\alpha f}$ ●, preceding start of plastic deformation of martensite ○, consequently no point of inflextion *x*.

temperature dependence. It is, however, raised considerably by the ausforming-induced defects.

$$\Delta\sigma_{p\alpha} = C_\alpha G_\alpha b_\alpha \sqrt{\varrho_\alpha} \tag{5}$$

The course of a stress–strain curve, especially the existence of a range of purely elastic deformation of martensite $\varepsilon_{e\alpha}$, depends on the condition:

$$\sigma_{\beta\alpha f} \lesseqgtr \sigma_{p\alpha} \tag{6a}$$

A low test temperature, not too far above M_s, and considerable work hardening by ausforming favors the condition:

$$\sigma_{\beta\alpha f} \ll \sigma_{p\alpha} \tag{6b}$$

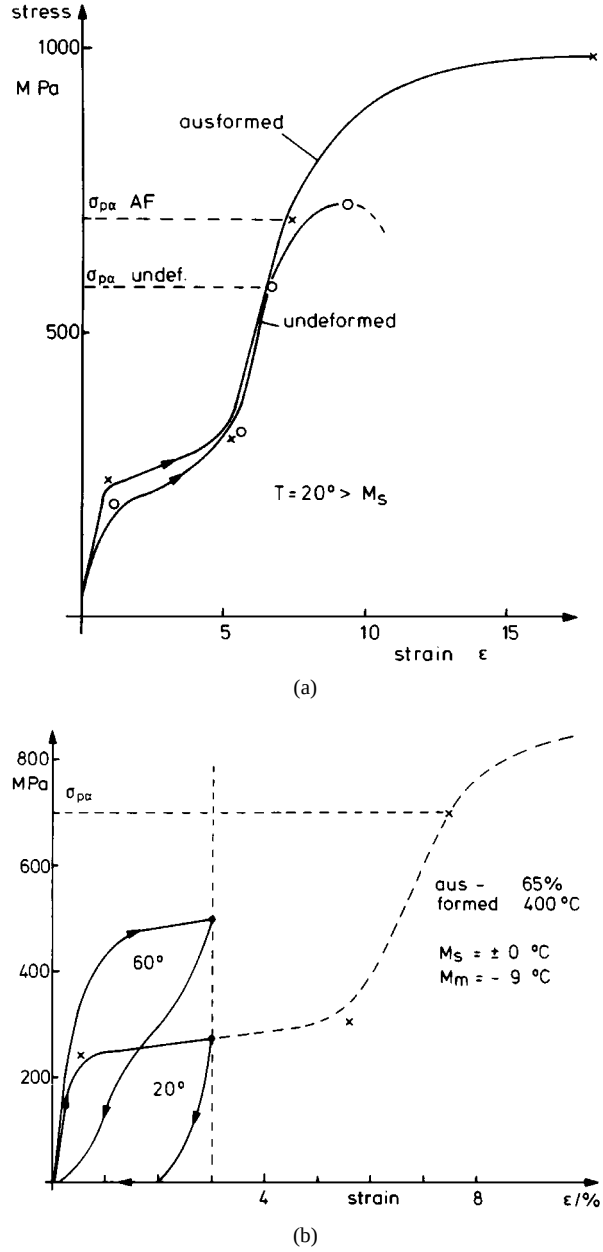

Figure 9 (a) Stress-strain curves of untreated and AF-treated alloy, compare Table I; and (b) 3%-pseudo-elastic (60 °C) or -plastic (20 °C) yielding of ausformed alloy.

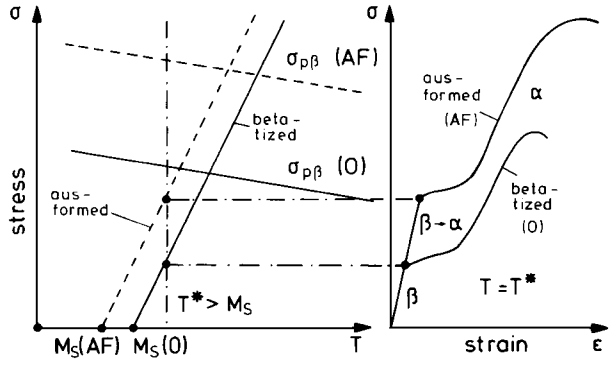

Figure 10 Effects of ausforming on martensite start M_s and pseudo-yield stress $\sigma_{\beta\alpha}$, schematic.

and therefore the separation of the range of stress-induced transformation and of true plasticity (Fig. 14). The untreated condition shows a point of inflection

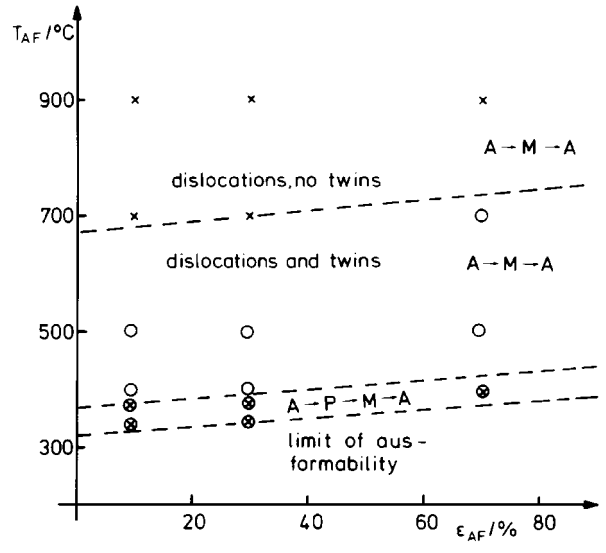

Figure 11 Effect of ausforming conditions (T_{AF}, ε_{AF}) on microstructure and mode of transformation *x* dislocations; ○ plus twins, ⊗ plus particles; A austenite; M martensite, p premartensite.

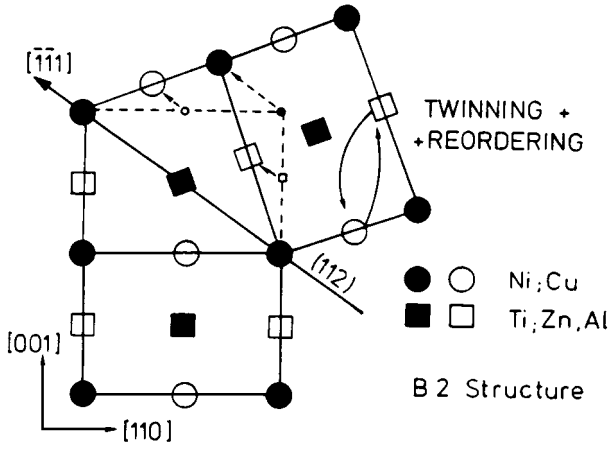

Figure 12 Model for a combined twinning + reordering reaction in the B2-structure.

$d^2\sigma/d\varepsilon^2$ at which the alloy is still transforming, while the martensite is already plastically deforming:

$$\sigma_{\beta\alpha} > \sigma_{p\alpha} \tag{6c}$$

Condition 6b is required for most shape memory applications, especially if repeated transformation cycles are required. Condition 6c implies that undesired defects originate and consequently fatigue phenomena occur (Figs 5, 11 and 12) [11–14]. These lead not only to mechanical damage and final fracture but also to uncontrolled shifts in transformation temperatures and reductions in the SM-effects.

Research on precipitation and textures produced by ausforming and fatigue resistance is under way. Based on this understanding, a further improvement of shape memory as well as conventional mechanical properties is expected, which is one prerequisite for safe performance of these materials in engineering and medicine (Figs 13 and 14) [14].

Acknowledgements

Thanks are due to Mr K. Rittner, who conducted the experimental work, especially the thermomechanical treatments and to Mr J. Spielfeld (mechanical testing) as well as to Mrs I. Wittkamp, Dr G. Kubla (TEM), Mr E. Kobus (SEM), and Mr M. Hühner, who helped with the metallographic work. This work was supported by the Volkswagenstiftung (VW foundation I/70283).

References

1. V. F. ZACKEY, *et al*., in "The Relation between Microstructure and Mechanical Properties," (H. M. S. O., London, 1963) p. 847.
2. E. HORNBOGEN, in "Innovation in Ultra High Strength Steel Technology," edited by G. B. Olson Proceedings of the thirtyfourth Sagamore Conference, Lake George, NY (1983) p. 113.
3. M. THUMANN and E. HORNBOGEN, *Z. Met. kd.* **79** (1988) 119.
4. M. FRANZ and E. HORNBOGEN, *ibid.* **86** (1995) 31
5. E. HORNBOGEN, in "Engineering Aspects of SMA," edited by T. W. DUERIG *et al*. (Butterworth, London, 1990) pp. 267–280.
6. E. HORNBOGEN and E. KOBUS, *Prakt. Metallogr*. **30** (1993) 507.
7. R. W. CAHN and J. A. COLL, *Acta Metall*. **9** (1961) 138.
8. M. J. MARCINKOWSKI, in "Electron Microscopy and Strength of Crystals," edited by G. Thomas and J. Washburn (Wiley, NY, 1963) p. 333.
9. E. HORNBOGEN, *Acta Metall*. **33** (1985) 595.
10. E. HORNBOGEN, in "Micromechanisms of Advanced Materials," edited by S. N. G. Chun *et al*., (T. M. S. Warrendale, Pa, 1995) p. 307.
11. K. N. MELTON and O. MERCIER, *Scr. Metall.* **13** (1970) 73.
12. J. PERKINS and W. E. MUESING, *Metall. Trans. A.* **14** (1983) 93 and *Acta Metall*. **27** (1979) 137.
13. M. SADE and E. HORNBOGEN, *Z. Metallkde*. **79** (1988) 678.
14. E. PATOOR and M. BERVEILLER (Eds), "Technologie des Alliages à Mémoir de Forme," (Hermes, Paris 1994).

Received 31 July 1997
and accepted 28 July 1998